Journal of ELECTRONIC MATERIALS, Vol. 48, No. 9, 2019
https://doi.org/10.1007/s11664-019-07416-y

Optimum Design, Heat Transfer and Performance Analysis for Thermoelectric Energy Recovery from the Engine Exhaust System

YOUSEF S.H. NAJJAR[1,2] and AHMED SALLAM[1]

1.—Jordan University of Science and Technology, Irbid, Jordan. 2.—e-mail: y_najjar@hotmail.com

Thermoelectric waste heat recovery can improve the thermal efficiency of internal combustion engines and reduce CO_2 emissions. In this study, a mathematical optimization using a genetic algorithm method is applied to obtain the optimal fin parameters of a rectangular offset-strip fin heat exchanger, used with an automotive thermoelectric generator (TEG) system. Three fin parameters are considered (fin spacing, fin thickness and fin height). Their effect on the exhaust pumping power, the exhaust heat transfer coefficient and the system performance is explored. The main goal is to maximize the net power output of the system. Results show that fin spacing has the most significant effect on the system performance. Moreover, when fin spacing is reduced below 0.5 mm, a negative net power output is obtained. By comparing the performance of stainless-steel (SS) and copper heat exchangers, it was found that the SS heat exchanger requires smaller fin spacing and fin height, which induces a higher pressure drop. TEGs with higher maximum operating temperature will allow further utilization of the exhaust heat, without a decline in performance due to overheating. Finally, a maximum net power output of 553.3 W is achieved using the copper heat exchanger and commercial bismuth-telluride (Bi_2Te_3) thermoelectric modules.

Key words: Thermoelectric generators, automotive waste heat recovery, heat exchanger optimization, net power output, rectangular offset-strip fin

List of Symbols

A	Area (m^2)
C_p	Specific heat capacity (J/kg K)
D_h	Hydraulic diameter (m)
f	Friction factor
h	Heat transfer coefficient (W/m^2 K)
I	Current (A)
ji	Colburn factor
k	Thermal conductivity (W/m K)
L	Length (m)
m	Mass flow rate (g/s)
Nu	Nusselt number
W	Power (W)
P	Pressure (pa)
Pr	Prandtl number
Q	Volumetric flow rate (m^3/s)
q	Heat flow rate (W)
R	Electrical resistance (Ω)
Re	Reynolds number
S	Seebeck coefficient (V/K)
T	Temperature (K)
E	Voltage (V)
V	Velocity (m/s)

Greek Symbols

η	Efficiency (%)
ρ	Density (kg/m^3)
μ	Dynamic viscosity (kg/m s)

Subscripts

c	Cold
e	Electrical
f	Fin
g	Exhaust gas
h	Hot

(Received April 10, 2019; accepted June 29, 2019; published online July 8, 2019)

HX Heat exchanger
L Load
m Module
p Pumping
w Water

Abbreviations

TEG Thermoelectric generator
ROSF Rectangular offset-strip fin

INTRODUCTION

Automotive internal combustion engines utilize 30–40% of the fuel energy; the rest is lost as heat. Around 30–45% of it is expelled to the atmosphere through the exhaust system and the radiator. Waste heat recovery is the most direct and practical method to increase the overall efficiency of the vehicle, and thus improve fuel value and reduce harmful emissions to the atmosphere. With the increase in energy demand and the expected shortage of fossil fuel, the need for sustainable resources grows. Hence, this was initially handled by using clean fuels,[1] utilization of waste heat[2–6] and adopting different configurations where resources and environment are conserved.

Recent research in waste heat recovery has focused on thermoelectric recovery, where thermal energy is directly converted to electrical energy using thermoelectric generators (TEGs). TEGs are solid-state devices that operate on the Seebeck effect phenomenon. When a temperature difference is applied on the opposite sides of a thermoelectric module, electrical power is produced directly. These devices have attracted great attention for their waste heat recovery potential, due to numerous advantages, such as the absence of moving parts, compactness and long operating life.

In et al.[7] developed a mathematical model to predict the effect of varying relevant factors on the performance of an automotive TEG system. Among these factors were the exhaust flow rate and temperature. They reported that for the case of water-cooled TEGs, increasing the heat transfer coefficient of the hot side will greatly improve the power output. Thus, heat transfer enhancement is critical for improving the system performance.

Thacher et al.[8] conducted experimental tests on a TEG system installed in a 1999 GMC Sierra truck. A rectangular offset-strip fin (ROSF) heat exchanger was used for heat transfer enhancement. They reported that an overall improvement in fuel efficiency was on the order of 1–2%. Lu et al.[9] investigated the effect of two types of heat transfer enhancements, an ROSF heat exchanger and metal foams, on the performance of a TEG system. It was found that metal foams provide better heat transfer enhancement but induce high pressure drop, resulting in a lower net power output. In et al.[7] investigated the performance of a TEG system with different heat sink shapes for heat transfer enhancement. They found that the power generation was greatest when a rectangular heat sink pillar was used. A 6.2-W power output for each module under the highest load condition was achieved. Kempf and Zhang[10] optimized a parallel-plate fin heat exchanger to obtain the highest fuel efficiency improvement. A 2.5% and 2.0% improvement was obtained for SiC and SS 444 heat exchangers, respectively. Kim et al.[11,12] carried out a series of numerical simulations to obtain the optimum fin thickness and number in a TEG system equipped with customized thermoelectric modules. The system performance was experimentally studied at the optimum conditions. A maximum power output of 119 W at 2000 rpm was achieved. Other types of heat enhancement techniques can be found in the literature, such as heat pipes,[13,14,15] microchannels[16] and using annular configurations.[17]

However, existing literature hasn't carefully considered each geometrical parameter of a heat exchanger separately, in order to fully understand its specific effects on the system performance. In this work, a numerical model was formulated for an automotive TEG system, where heat transfer enhancement is achieved by a ROSF heat exchanger. The goal is to obtain the maximum net power output from the system by optimizing the heat exchanger design. This is achieved by maximizing the electrical power output of the system, while minimizing the parasitic losses due to the heat exchanger weight and the pressure drop of the exhaust and cooling water.

THEORETICAL ANALYSIS

The mathematical model is based on HZ-20 thermoelectric modules commercially available from HI-Z Technology.[18] These modules perform well in the exhaust temperature range, and have a high power output compared to other commercial TEGs.

Properties of the module are shown in Table I. These properties are available in the product data sheet provided by the manufacturer.

Table I. HZ-20 module properties at design point and matched load

Physical properties	Value
Width and length	7.5 cm
Thickness	0.508 cm
Number of legs	142
Thermal properties	Value
Thermal conductivity	0.024 W/cm K
Heat flux	9.54 W/cm^2
Electrical properties	Value
Power	19 W
Internal resistance	0.3 Ω
Efficiency	4.5%

Figure 2 is a computer-aided design (CAD) model for the TEG system. Thirty HZ-20 modules are connected in series and mounted on the heat exchanger, 15 on each side with a 5×3 array configuration. The heat exchanger length and width are 450 mm and 250 mm, respectively, and they are fixed and were chosen to accommodate the 15 modules on each side. The heat exchanger height isn't fixed, and it is one of the parameters of optimization. The hot side of the module is heated by the exhaust gas, where the cold side is cooled by the engine cooling water, as shown in Fig. 1. The exhaust and the coolant are in a counter-flow configuration to enhance the heat transfer process. This design is based on previous work.[8]

It should be noted that since the cooling is achieved by the engine cooling water, the additional cooling load may require a larger radiator to provide sufficient cooling for both the engine and the TEG system.

Thermoelectric Generator

To simplify the analysis, the following assumptions were made: thermal resistance of air caused by gaps and imperfections is neglected, the thermal resistance of metallic conductors is neglected, the temperature along the hot and cold sides of the module is uniform, and ohmic heating occurs exclusively within the semiconducting legs.[19]

Thermoelectric modules are composed of two pellets of dissimilar semiconducting materials, an n-type and a p-type material, joined at their ends as shown in Fig. 3. A current that is proportional to the heat flux through the material and its respective Seebeck coefficient will flow through the circuit.

The Seebeck coefficient is a material property that represents the proportionality between induced voltage and temperature difference across the material. The International System of Units (SI) unit of the Seebeck coefficient is volts per kelvin, V/K.[20]

$$S = \frac{\Delta E}{\Delta T} \tag{1}$$

where S is Seebeck coefficient, and ΔV and ΔT are the voltage and temperature gradients, respectively. The established voltage will drive a current that will induce heat generation at one junction and heat absorption at the other; this phenomenon is known as the Peltier effect. As shown in Eq. 2, the amount of heat absorbed or rejected is directly related to the Seebeck coefficient of the material.

$$q = IST \tag{2}$$

where q is the rate of heat absorption or rejection, and I is the electrical current output. The heat transfer process is illustrated in Fig. 2. Where heat is transferred by conduction, the Peltier effect and ohmic heating occur. A steady-state one-dimensional energy balance is performed on the thermoelectric module; heat input and output at each side can be expressed as:

$$q_{\mathrm{h}} = \frac{k\Delta T}{L}(T_{\mathrm{h}} - T_{\mathrm{c}}) + IST_{\mathrm{h}} - \frac{I^2R_{\mathrm{e}}}{2} \tag{3}$$

$$q_{\mathrm{c}} = \frac{k\Delta T}{L}(T_{\mathrm{h}} - T_{\mathrm{c}}) + IST_{\mathrm{c}} + \frac{I^2R_{\mathrm{e}}}{2} \tag{4}$$

where q_{h} and q_{c} are the heat transfer rates at the hot and cold side respectively, T_{h} and T_{c} are the temperatures of the hot and cold side of the module, respectively, k is the thermal conductivity of the module, L is the module thickness and R_{e} is the internal electrical resistance of the module.

The electrical power output for each module equals

$$W_{\mathrm{m}} = q_{\mathrm{h}} - q_{\mathrm{c}} \tag{5}$$

Heat absorbed at the hot side from the exhaust gas by convection can be expressed as

$$q_{\mathrm{h}} = h_{\mathrm{g}}A_{\mathrm{h}}\left(\left(T_{\mathrm{g,in}} + T_{\mathrm{g,out}}\right)/2 - T_{\mathrm{h}}\right) \tag{6}$$

Similarly, for the heat rejected at the cold side to the cooling water by convection can be expressed as

$$q_{\mathrm{c}} = h_{\mathrm{w}}A_{\mathrm{c}}\left(T_{\mathrm{c}} - \left(T_{\mathrm{w,in}} + T_{\mathrm{w,out}}\right)/2\right) \tag{7}$$

where h_{g} and T_{g} are the exhaust gas heat transfer coefficient and temperature respectively. h_{w} and T_{w} are the cooling water heat transfer coefficient and temperature respectively. A_{h} and A_{c} are the effective areas of heat transfer with the exhaust gas and the cooling water respectively.

Accounting for the temperature change in the exhaust and the cooling water, we can obtain

$$q_{\mathrm{h}} = m_{\mathrm{g}}cp_{\mathrm{g}}\left(T_{\mathrm{g,in}} - T_{\mathrm{g,out}}\right) \tag{8}$$

$$q_{\mathrm{c}} = m_{\mathrm{w}}cp_{\mathrm{w}}\left(T_{\mathrm{w,out}} - T_{\mathrm{w,in}}\right) \tag{9}$$

where m is the mass flow rate and cp is the specific heat capacity. The total electrical power output and efficiency of the TEG system equals

$$W_{\mathrm{tot}} = 5\sum_{i=1}^{6} W_{\mathrm{m}} = I^2R_{\mathrm{L}} \tag{10}$$

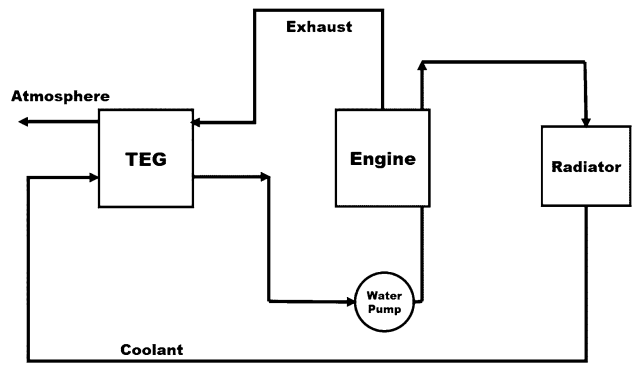

Fig. 1. Schematic of the automotive TEG system.

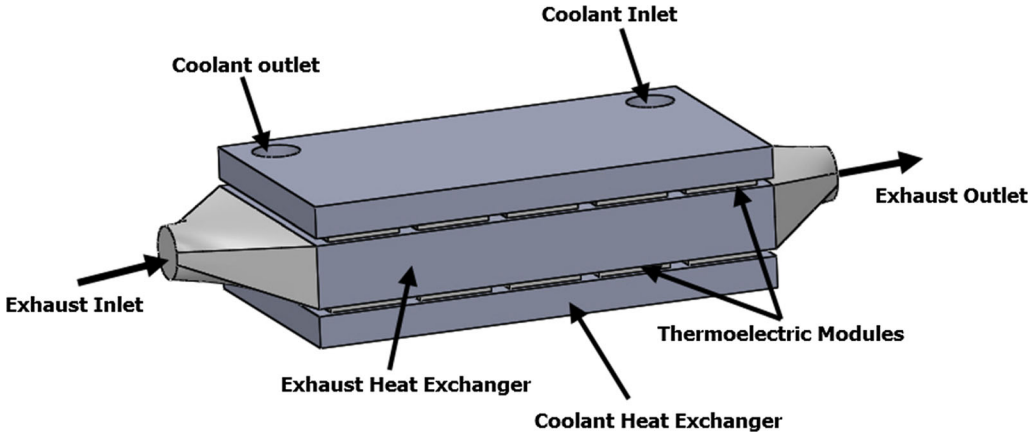

Fig. 2. CAD model for the TEG system installed on the vehicle exhaust system.

$$\eta = W_{\text{tot}}/q_{\text{h,tot}} \tag{11}$$

where R_{L} is the load electrical resistance and $q_{\text{h,tot}}$ is the total heat transfer rate to the system. $q_{\text{h,tot}}$ is given by

$$q_{\text{h,tot}} = 5\sum_{i=1}^{6} q_{\text{h}}. \tag{12}$$

Exhaust Heat Exchanger

Since the heat transfer coefficient of the exhaust gas is very low (20–80 W/(m^2 K)[21]), the area of heat exchange is limited to the surface area of the thermoelectric modules. This will limit the hot-side temperature of the module and, consequently, limit the TEG performance. Thus, a ROSF heat exchanger is chosen to enhance the heat transfer process between the exhaust gas and the thermoelectric modules.

Due to the ROSF heat exchanger's high heat transfer performance and compactness,[22] it is widely used in automotive heat recovery systems.

As shown in Fig. 3, the geometry of the ROSF heat exchanger is defined by fin spacing s_{f}, fin thickness t_{f}, fin height h_{f} and fin length l_{f}.

The Colburn factor and the friction factor for an ROSF heat exchanger can be calculated using the following correlations provided by Magnlik and Bergles[23] (Fig. 4):

$$ji = 0.6522Re^{-0.5403}\left(\frac{s_{\text{f}}}{h_{\text{f}}}\right)^{-0.1541}\left(\frac{t_{\text{f}}}{l_{\text{f}}}\right)^{0.1499}\left(\frac{t_{\text{f}}}{s_{\text{f}}}\right)^{-0.0678}$$
$$\left\{1 + 5.269\times 10^{-5}Re^{1.340}\left(\frac{s_{\text{f}}}{h_{\text{f}}}\right)^{0.504}\left(\frac{t_{\text{f}}}{l_{\text{f}}}\right)^{0.456}\left(\frac{t_{\text{f}}}{s_{\text{f}}}\right)^{-1.055}\right\}^{0.1} \tag{13}$$

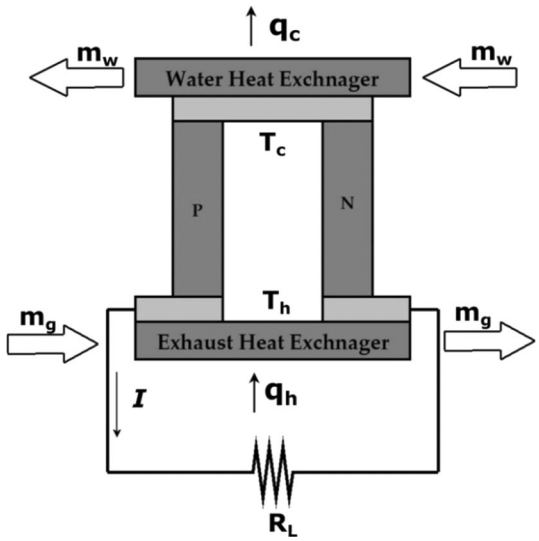

Fig. 3. Schematic illustration for the heat transfer process of a simplified thermoelectric module.

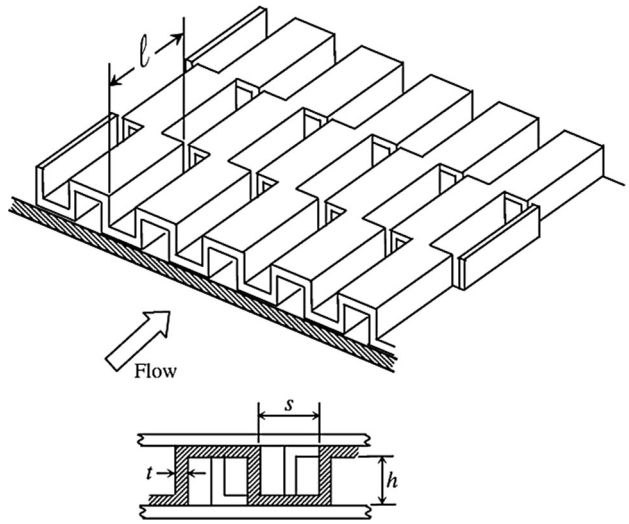

Fig. 4. Geometry of an ROSF heat exchanger. Reprinted with permission of Ref. 24.

$$f_g = 9.6243Re^{-0.7422}\left(\frac{s_f}{h_f}\right)^{-0.1856}\left(\frac{t_f}{l_f}\right)^{0.3053}\left(\frac{t_f}{s}\right)^{-0.2659}\left\{1 + 7.6669\times10^{-8}Re^{4.429}\left(\frac{s_f}{h_f}\right)^{0.92}\left(\frac{t_f}{l_f}\right)^{3.767}\left(\frac{t_f}{s_f}\right)^{0.236}\right\}^{0.1} \quad (14)$$

where Re is the Reynolds number and is given by

$$Re = \frac{\rho_g V_g D_h}{\mu_g} \quad (15)$$

where ρ_g, v_g and μ_g are the exhaust gas density, velocity and viscosity, respectively. D_h is the hydraulic diameter and is given by

$$D_h = \frac{4A_{section}}{A/l_f} = \frac{4s_f h_f l_f}{2(s_f h_f + h_f l_f + t_f h_f) + t_f s_f} \quad (16)$$

Fin efficiency is defined by

$$\eta_f = \frac{\tanh(m_f l_f)}{m_f l_f} \quad (17)$$

where m_f equals

$$m_f = \sqrt{\frac{2h_g(t_f + l_f)}{k_f l_f t_f}} \quad (18)$$

where k_f is the thermal conductivity of the heat exchanger material.

The Nusselt number of the exhaust gas can be estimated by

$$Nu_g = jiRePr^{1/3} \quad (19)$$

The exhaust gas pressure drop across the hot heat exchanger and the corresponding power that is required for pumping can be expressed as[11]

$$\Delta P_g = 4f_g\rho_g\left(\frac{L_{HX}}{D_h}\right)\left(\frac{v_g^2}{2}\right) \quad (20)$$

$$P_{p,g} = \Delta P_g Q_g \quad (21)$$

where L_{HX} is the heat exchanger length and Q_g is the exhaust gas flow rate.

Cooling Water Heat Exchanger

The coolant heat exchanger consists of 12 parallel channels, 6 on each side with equal rectangular cross-sectional area.[20] The Nusselt number for the cooling water can be estimated using the Dittus–Boelter equation[19]:

$$Nu_w = 0.023RePr^{0.4} \quad (22)$$

The pressure drop is estimated by

$$\Delta W_w = 4f_w\rho_w\left(\frac{L_{HX}}{D_h}\right)\left(\frac{V_w^2}{2}\right) \quad (23)$$

where f_w is the Darcy resistance coefficient and is given by[9]

$$f_w = (1.82\ln(Re) - 1.62)^{-2} \quad (24)$$

The required water pumping power can be expressed as

$$W_{P,w} = Q_w\Delta W_w. \quad (25)$$

Power Loss Due to System Weight

The power lost due to the total weight of the TEG system is given by

$$W_{weight} = \mu V w_{sys}/\eta \quad (26)$$

where μ is the rolling resistance coefficient, V is the vehicle velocity, W_{sys} is the weight of the hot and cold heat exchangers including the modules and η is the driveline transmission efficiency. μ and η are taken to be 0.012 and 0.9, respectively.[25]

Optimization

The performance of the TEG system is evaluated by the net power output, since it is the actual useful power added to the vehicle. Equation 26 shows that to maximize the net power output, a maximum electrical power output must be obtained from the thermoelectric modules with minimum power loss due to the pressure drop and the system weight.

$$W_{net} = W_{tot} - W_{p,g} - W_{P,w} - W_{weight} \quad (27)$$

Therefore, mathematical optimization using a genetic algorithm method was performed on an ROSF heat exchanger to achieve the optimal design for the highest net power output. Moreover, three fin parameters were selected as design variables, which are fin spacing s_f, fin thickness t_f and fin height h_f, as shown in Table II. Both copper and stainless steel (SS) were considered as heat exchanger material, as shown in Table III, both of which are wildly used for heat-enhancement applications due to their high thermal conductivity and stability.

Since the total width of the heat exchanger is fixed, the number of fins will vary according to the corresponding fin thickness and spacing.

The optimization was performed for highway driving conditions, since it is important to optimize the TEG system during its highest potential for electrical power production, due to higher exhaust

Table II. Fin optimization parameters

Parameter	Symbol	Range (mm)
Fin thickness	t_f	0.1–8
Fin spacing	s_f	0.5–8
Fin height	h_f	30–80

Table III. Properties of the heat exchanger materials

Material	Density (g/cm^3)	Thermal conductivity (W/m K)
Copper	8.94	400
Stainless steel	7.81	16.7

Table IV. Mean inlet conditions measured under highway driving conditions

Parameter	Value
Exhaust gas inlet temperature	708 (°C)
Exhaust gas inlet flow rate	21.9 (g/s)
Cooling water inlet temperature	82.0 (°C)
Cooling water flow rate	14.9 (L/min)

temperature and flow rate. The mean inlet conditions for the exhaust gas and the cooling water for a 2.0-L 4-cylinder vehicle at a speed of 107 km/h under highway driving conditions were experimentally obtained by Ref. 10 and are shown in Table IV.

Since the actual driving conditions of vehicles are unsteady, it is challenging to design and optimize a TEG system that performs well under complex driving conditions. The effect of vehicle driving conditions on a similar thermoelectric heat recovery system has been studied.[26] It was found that acceleration and deceleration of the vehicle will have a noticeable effect on the convective heat transfer at the hot and cold side of the system. As a result, this will significantly affect the performance and power output of the system. It has also been suggested that a highly frequent change in driving conditions may have a negative effect on the TEG performance.

Validation

To verify the validity of the mathematical model developed in this study, the heat exchanger geometry, the exhaust gas inlet parameters, the cooling water inlet parameters and the number of thermoelectric modules are adjusted to fit the experiment done by Thacher.[9] The results are then obtained from our mathematical model and compared with the experimental power measurements, as shown in Fig. 5.

As it can be seen in Fig. 5, at low velocities, there is a strong agreement between the numerical results and the experimental results. However, as the velocity increases beyond 48.3 km/h, the difference between the experimental results and the numerical results starts to increase significantly up to 34%. This can be due to the following reasons: the difference between the thermoelectric properties

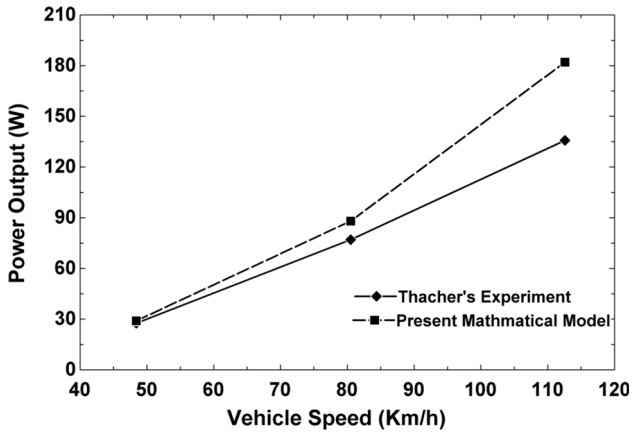

Fig. 5. Comparison between the numerical and experimental results of the TEG system's power output.

used in the mathematical model and the properties of the actual thermoelectric modules, the assumptions of uniform heat distribution and uniform surface temperature distribution over the thermoelectric modules deviate from the actual case as the speed of the vehicle increase due to the increase in the exhaust flow rate and temperature.

RESULTS AND DISCUSSION

In this section, we will review the effect of each fin geometrical parameter on: the exhaust gas heat transfer coefficient, the required exhaust pumping power due to the pressure drop at the heat exchanger and, finally, on the total and net power output to evaluate the system performance.

To study the effect of each parameter carefully, each parameter will be varied separately, while the other two parameters will be fixed at their optimal values.

Table V summarizes the optimization results for each heat exchanger material. A higher pressure drop and heat transfer coefficient is expected in the SS heat exchanger since it has smaller optimal fin spacing and fin height.

Fin Spacing Effect

As shown in Fig. 6a and b, when fin spacing is decreased, an increase in the exhaust heat transfer coefficient and pumping power is observed, due to higher exhaust flow speed. Decreasing the fin spacing from 5 mm to 0.5 mm will increase the heat transfer coefficient by 300%, while an exponential increase is observed for fin spacings below 0.5 mm. Smaller fin spacing and consequently a higher heat transfer coefficient will increase the hot-side temperature and the power output of the system. However, when fin spacing is reduced below 0.5 mm, a rapid increase in pressure drop and pumping power occurs, at a rate that exceeds the increase in power output. As a result, the net power output of the system declines rapidly and becomes

negative, as shown in Fig. 6c and d. Not only no enhancement to the vehicle power is achieved, but the system will actually consume power from the engine and decrease its efficiency. It is clear that the optimal fin spacing for the SS heat exchanger is smaller than that of the copper one; this can be attributed to the significantly lower thermal conductivity of SS. The smaller fin spacing in the SS heat exchanger will provide a higher heat transfer coefficient to achieve sufficient heat transfer rate to the modules.

It is generally true that a higher heat transfer coefficient is desired to achieve higher hot-side temperature and higher power output. However, as Fig. 6c and d show, when fin spacing is decreased below the optimal values, the power output starts to decline, due to the overheating of the thermoelectric modules. When the heat transfer coefficient exceeds a certain value, the hot-side temperature becomes higher than that of the operating design temperature. As a result, the Seebeck coefficient of the modules decreases, and their thermal conductivity increases. This will lower the modules' performance and power output, as shown in Eq. 5.

Table V. Optimization results for the copper and SS heat exchangers

Parameter	Copper	SS
Net power output (W)	553.5	548.9
Fin spacing (mm)	3.966	1.616
Fin thickness (mm)	0.1216	0.1467
Fin height (mm)	44.12	32.67

Fin Thickness Effect

As shown in Fig. 7a and b, the exhaust heat transfer coefficient and pumping power increase as the fin thickness is increased, due to higher flow speed. Increasing the fin thickness to 1 mm will increase the heat transfer coefficient by approximately 65%. However, fin thickness effect on the pumping power is very small in the SS heat exchanger and negligible in the copper heat exchanger.

As shown in Fig. 7c and d, with very thin fins (below 0.1 mm), the power output drops rapidly, due

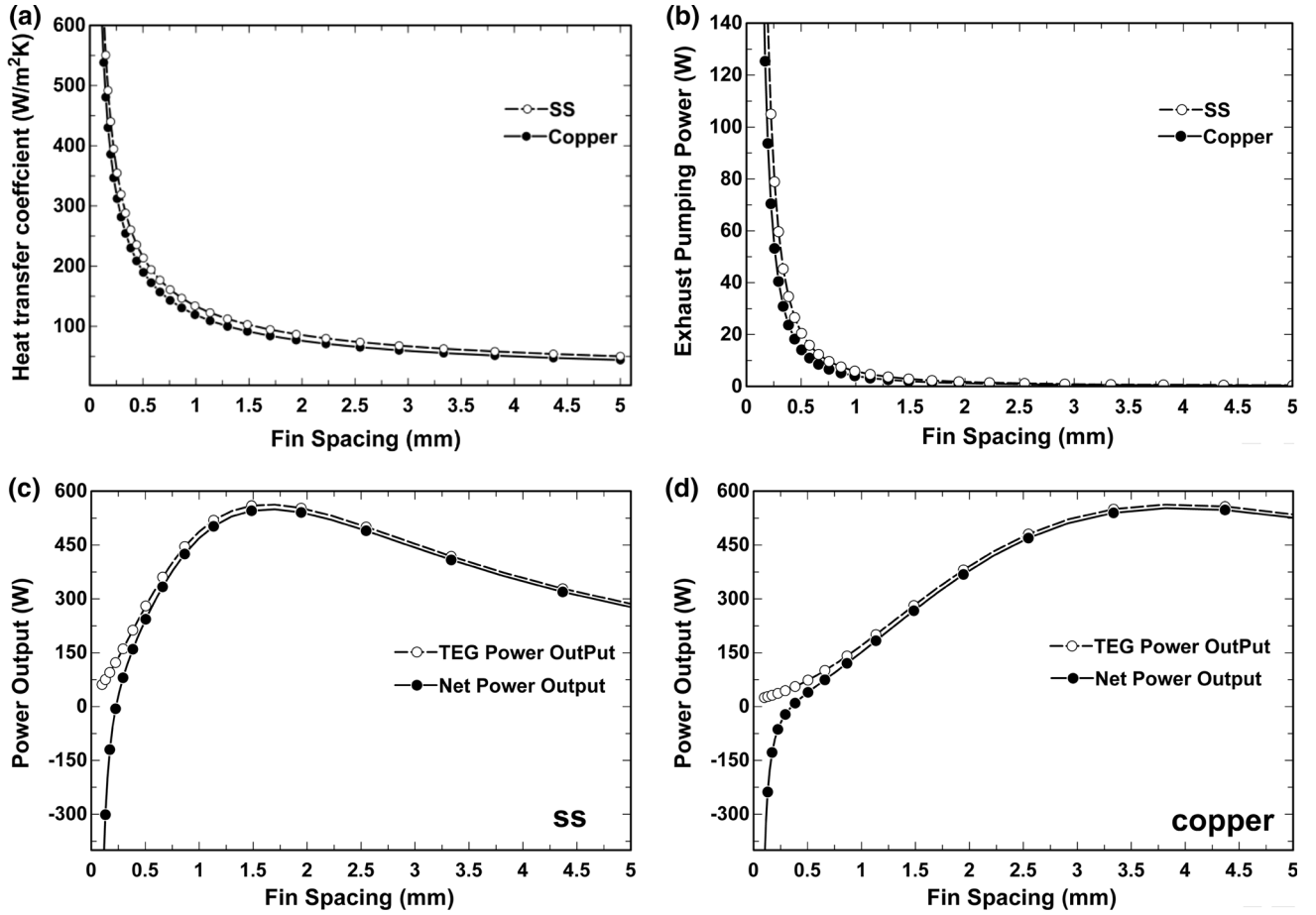

Fig. 6. (a) Heat transfer coefficient and (b) exhaust pumping power as a function of fin spacing at the optimal fin height and fin thickness. TEG power output and net power output for the (c) SS and (d) copper heat exchangers as a function of fin spacing at the optimal fin height and fin thickness.

to the decrease in fin efficiency, as shown in Eqs. 17 and 18. Low fin efficiency leads to a decrease in the effective area of heat exchange.

Despite the increase in the heat transfer coefficient as fin thickness increases, the power output is decreased by 14% and 4% in the SS and copper heat exchangers, respectively. Since the heat exchanger width is fixed, higher fin thickness will result in fewer fins and smaller heat transfer area leading to a lower hot-side temperature. Note that in the SS heat exchanger, the decrease in the power output is more rapid due to the lower thermal conductivity.

The lost power which is the difference between the TEG power output and the net power output continues to increase as the fin thickness is increased. This is mainly due to the increase in the system weight since the increase in pumping power is negligible.

Fin Height Effect

To optimize the fin height, a balance between the heat transfer area and the heat transfer coefficient must be achieved. A significant reduction in either will result in a lower hot-side temperature and lower power output. As expected, the exhaust heat transfer coefficient and pumping power will increase as the fin height decreases due to higher flow speed, as shown in Fig. 8a and b. It is also noted that the fin height effect on the power output is small for fin heights above 25 mm. Only a 2% reduction is observed in the SS heat exchanger, while it is almost constant in the copper heat exchanger, as evident in Fig. 8c and d. For shorter fin heights (below 25 mm), the power output starts to decline due to insufficient area of heat transfer.

If the design requires certain constraints on the system volume, fin height can be modified without sacrificing much power output, especially if the fin spacing and fin thickness were to be modified accordingly.

Heat Exchanger Design Considerations

In Fig. 9, the net power output of the TEG system is plotted as a function of fin thickness and fin spacing at the optimal fin height, and the maximum net power output point is highlighted. It is clear

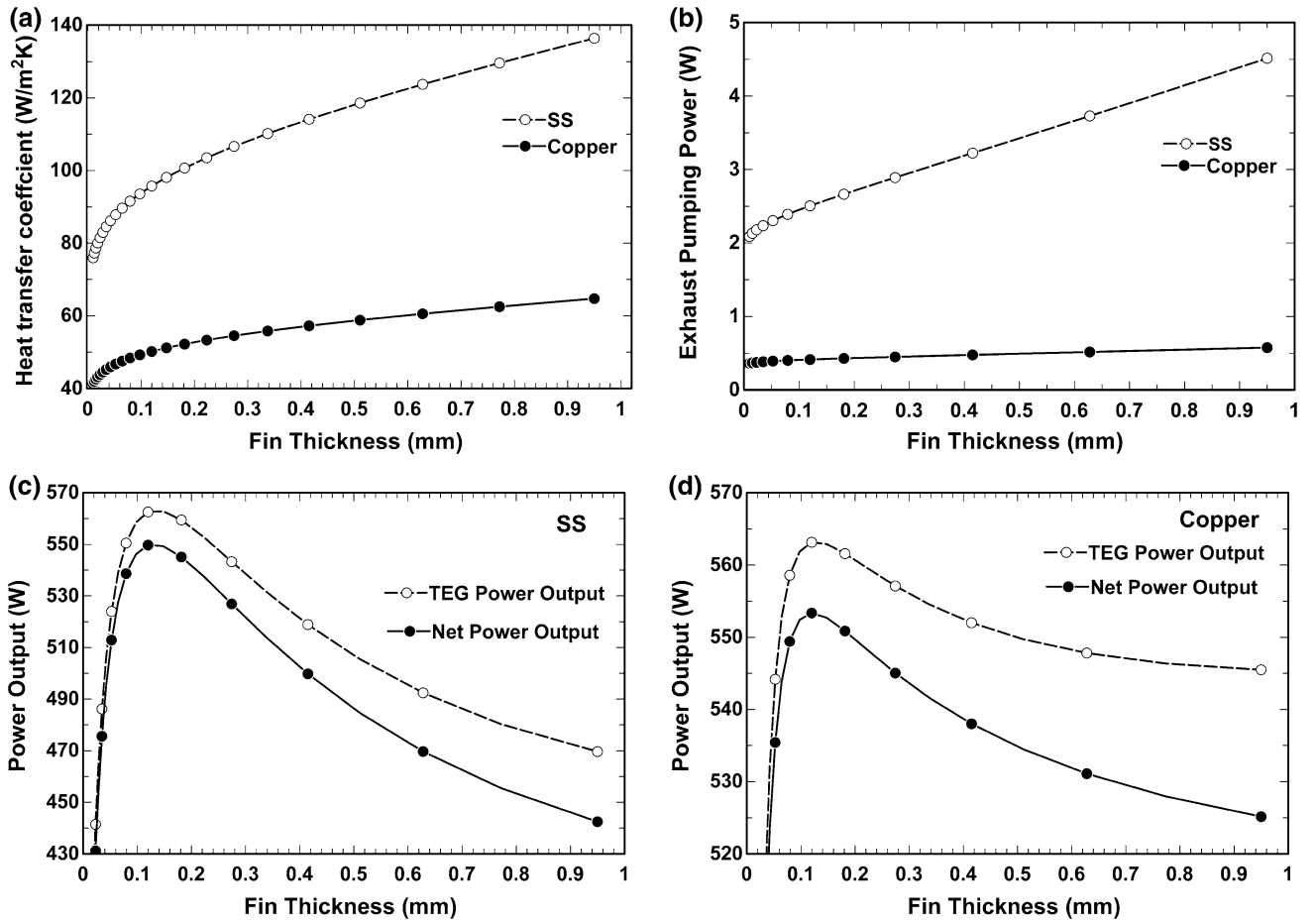

Fig. 7. (a) Heat transfer coefficient and (b) exhaust pumping power as a function of fin thickness at the optimal fin height and fin spacing. TEG power output and net power output for the (c) SS and (d) copper heat exchangers as a function of fin thickness at the optimal fin height and fin spacing.

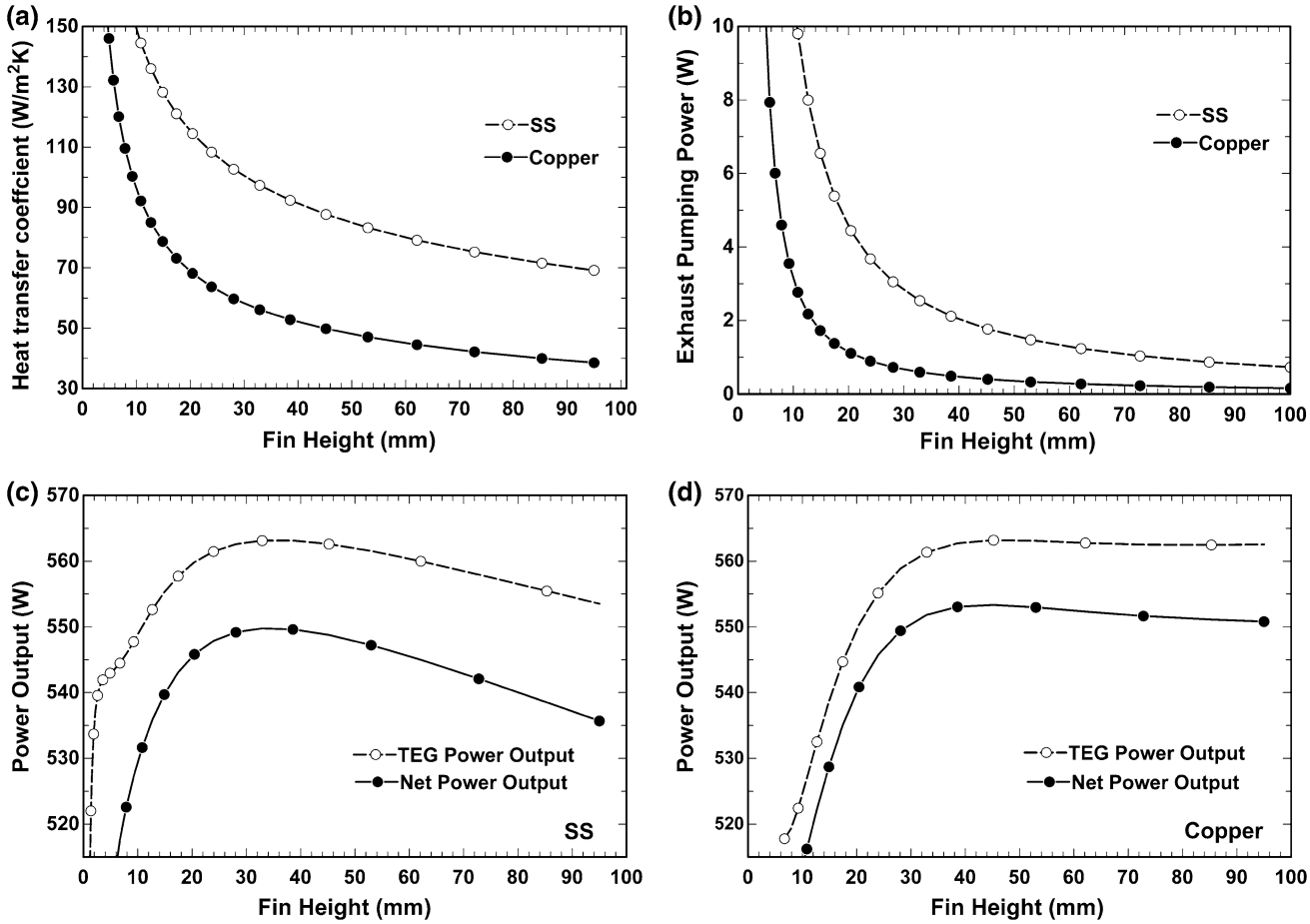

Fig. 8. (a) Heat transfer coefficient and (b) exhaust pumping power as a function of fin height at the optimal fin spacing and fin thickness. TEG power output and net power output for the (c) SS and (d) copper heat exchangers as a function of fin height at the optimal fin height and fin spacing.

from the figure that many combinations of fin spacing and fin thickness can achieve a net power output that is similar to the optimum value. The TEG system with the copper heat exchanger, a 5-mm fin spacing and a 0.6-mm fin thickness can achieve a net power output of 547.5 W, only 1% less than the maximum net power output. Also, for the SS heat exchanger, a fin spacing of 2.7 mm and a fin thickness of 0.62 mm will achieve a net power output of 545.5 W, only, 0.7% less than the maximum net power output.

Thus, it is possible to modify the design of the heat exchanger and alter the fin geometrical parameters from their optimal values (within a certain range) without sacrificing much power. The different combinations of fin parameters may have a cheaper manufacturing and material cost, or may achieve certain size and weight criteria that may not have been otherwise possible with the optimal parameters.

Moreover, it is observed that the system with the SS heat exchanger has a maximum net power output of only 1% less than that of the copper heat exchanger. The smaller fin height and fin spacing in the SS heat exchanger provide further enhancement to the heat transfer coefficient, which will overcome the lower thermal conductivity of the material and provide a sufficient heat transfer rate to the modules. Thus, a cheaper material with lower thermal conductivity can be used in the exhaust heat exchange without sacrificing much power output, if the system is optimized accordingly. However, with thermoelectric modules that can operate on a higher hot-side temperature, the thermal conductivity of the exhaust heat exchanger material will become more critical to the system performance. As such, these modules will have the potential to utilize the high thermal conductivity of the material without overheating. Ref. 25 showed that when thermoelectric modules that are designed for high-temperature applications are used, fuel efficiency improvement is 25% greater with a SiC heat exchanger compared to a SS 444 heat exchanger due to the lower thermally conductivity of SS 444.

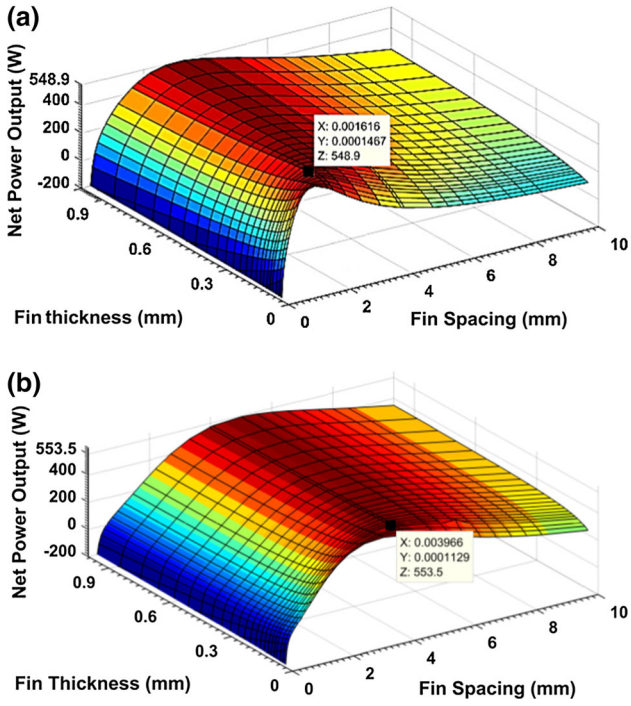

Fig. 9. Net power output as a function of fin thickness and spacing for the SS (a) and copper (b) heat exchangers at the optimal fin height.

CONCLUSIONS

1. maximum net power output of 553 W was achieved using the TEG system with the copper heat exchanger, with only 1% reduction when the SS heat exchanger is used.
2. Fin spacing effect on the exhaust pumping power and heat transfer coefficient as well as the net power output is much more significant than that of fin thickness and fin height. Thus, fin spacing should be carefully considered.
3. The optimal fin spacings for the copper and SS heat exchangers are 3.96 mm and 1.62 mm, respectively. The smaller fin spacing in the SS exchanger will provide higher heat transfer at the cost of higher pressure drop.
4. As the fin thickness is decreased, the exhaust heat transfer coefficient and pumping power increase. Decreasing the optimal fin spacing by 50% in the copper heat exchanger will increase the heat transfer coefficient by 45%, but it will have a negligible effect on the pumping power.
5. When the fin spacing is reduced below a critical value of 0.5 mm, the exhaust pumping power and heat transfer coefficient increase exponentially. This will result in a negative net power output and, consequently, a reduction in the engine efficiency.
6. When the exhaust heat transfer coefficient exceeds a certain value (75 W/m^2 K), the thermoelectric modules' performance starts to drop due to overheating. Hence, to obtain additional power gain, thermoelectric modules designed for higher temperatures are recommended.

ACKNOWLEDGMENTS

This research received no specific grant from any funding agency in the public, commercial or not-for-profit sectors.

REFERENCES

1. Y.S. Najjar, *Int. J. Hydrogen Energy* 38, 10716 (2013).
2. N.J. Lamfon, Y.S.H. Najjar, and M. Akyurt, *Fuel Energy Abstr.* 39, 51 (1998).
3. Y.S. Najjar, *Energy* 36, 4136 (2011).
4. N.M. Jubeh and Y.S. Najjar, *Energy* 38, 228 (2012).
5. Y. Najjar, M. Akyurt, O. Al-Rabghi, and T. Alp, *Heat Recovery Syst. CHP* 13, 471 (1993).
6. Y.S. Najjar and A.M. Radhwan, *Heat Recovery Syst. CHP* 8, 211 (1988).
7. B.D. In, H.I. Kim, J.W. Son, and K.H. Lee, *Int. J. Heat Mass Transf.* 86, 667 (2015).
8. E.F. Thacher, B.T. Helenbrook, M.A. Karri, and C.J. Richter, *Proc. Inst. Mech. Eng. D J. Automob. Eng.* 221, 95 (2007).
9. C. Lu, S. Wang, C. Chen, and Y. Li, *Appl. Therm. Eng.* 89, 270 (2015).
10. N. Kempf and Y. Zhang, *Energy Convers. Manag.* 121, 224 (2016).
11. T.Y. Kim, A.A. Negash, and G. Cho, *Energy Convers. Manag.* 124, 280 (2016).
12. T.Y. Kim, S. Lee, and J. Lee, *Energy Convers. Manag.* 124, 470 (2016).
13. B. Li, K. Huang, Y. Yan, Y. Li, S. Twaha, and J. Zhu, *Appl. Energy* 205, 868 (2017).
14. Q. Cao, W. Luan, and T. Wang, *Appl. Therm. Eng.* 130, 1472 (2018).
15. K. Huang, B. Li, Y. Yan, Y. Li, S. Twaha, and J. Zhu, *Appl. Therm. Eng.* 117, 501 (2017).
16. S. Krishnan, N.K. Karri, P.K. Gogna, J.R. Chase, J.-P. Fleurial, and T.J. Hendricks, *J. Electron. Mater.* 41, 1622 (2012).
17. S. Fan and Y. Gao, *Energy* 150, 38 (2018).
18. Hi-Z Technology, HZ-20 product data-sheet, http://hi-z.com/wp-content/uploads/2016/08/HZ-20-Datasheet.pdf.
19. F.P. Incropera, *Fundamentals of Heat and Mass Transfer* (Hoboken: Wiley, 2013).
20. M.A. Karri, Modeling of an Automotive Exhaust Thermoelectric Generator: A Thesis (2005).
21. J.-Y. Jang and Y.-C. Tsai, *Appl. Therm. Eng.* 51, 677 (2013).
22. W.M. Kays and A.L. London, *Compact Heat Exchangers* (Malabar: Krieger, 1998).
23. R.M. Manglik and A.E. Bergles, *Exp. Therm. Fluid Sci.* 10, 171 (1995).
24. H. Bhowmik and K.-S. Lee, *Int. Commun. Heat Mass Transf.* 36, 259 (2009).
25. M. Karri, E. Thacher, and B. Helenbrook, *Energy Convers. Manag.* 52, 1596 (2011).
26. S. Yu, Q. Du, H. Diao, G. Shu, and K. Jiao, *Energy Convers. Manag.* 96, 363 (2015).